Coulomb Blockade Anisotropic Magnetoresistance Effect in a (Ga, Mn)As Single-Electron Transistor

J. Wunderlich,[1] T. Jungwirth,[2,3] B. Kaestner,[4] A. C. Irvine,[5] A. B. Shick,[6] N. Stone,[1] K.-Y. Wang,[1] U. Rana,[4] A. D. Giddings,[3] C. T. Foxon,[3] R. P. Campion,[3] D. A. Williams,[1] and B. L. Gallagher[3]

[1]*Hitachi Cambridge Laboratory, Cambridge CB3 0HE, United Kingdom*
[2]*Institute of Physics ASCR, Cukrovarnická 10, 162 53 Praha 6, Czech Republic*
[3]*School of Physics and Astronomy, University of Nottingham, Nottingham NG7 2RD, United Kingdom*
[4]*National Physical Laboratory, Teddington T11 0LW, United Kingdom*
[5]*Microelectronics Research Centre, Cavendish Laboratory, University of Cambridge, CB3 0HE, United Kingdom*
[6]*Institute of Physics ASCR, Na Slovance 2, 182 21 Praha 8, Czech Republic*

(Received 30 March 2006; published 15 August 2006)

We observe low-field hysteretic magnetoresistance in a (Ga, Mn)As single-electron transistor which can exceed 3 orders of magnitude. The sign and size of the magnetoresistance signal are controlled by the gate voltage. Experimental data are interpreted in terms of electrochemical shifts associated with magnetization rotations. This Coulomb blockade anisotropic magnetoresistance is distinct from previously observed anisotropic magnetoresistance effects as it occurs when the anisotropy in a band structure derived parameter is comparable to an independent scale, the single-electron charging energy. Effective kinetic-exchange model calculations in (Ga, Mn)As show chemical potential anisotropies consistent with experiment and *ab initio* calculations in transition metal systems suggest that this generic effect persists to high temperatures in metal ferromagnets with strong spin-orbit coupling.

DOI: 10.1103/PhysRevLett.97.077201 PACS numbers: 75.50.Pp, 73.23.Hk, 75.47.−m, 85.75.Mm

Single electronics, which is based on the discrete charge of the electron [1], is the ultimate in miniaturization and electrosensitivity. Spintronics, which is based on manipulating electron spins [2], delivers high magnetosensitivity and nonvolatile memory effects. The potential of hybrid single-electronic–spintronic devices and the fundamental importance of spin phenomena at nanoscale have motivated a number of studies of spin transport in the Coulomb blockade (CB) regime [3–6]. Experiments in single-electron transistors (SETs) in which the leads and island comprise different ferromagnetic materials [3] have shown both electric and magnetic field dependent CB oscillations. These magneto-CB oscillations are due to the Zeeman energy changing the relative chemical potentials in the leads and in the island. They occur at high applied fields and are nonhysteretic. A small low-field hysteretic magnetoresistance (MR) effect has been demonstrated in SETs when the relative orientation of the magnetization of the leads is switched from parallel to antiparallel [3,6]. Here the response to the magnetic field is attributed to subtle, spin-coherent resonant tunneling effects through quantized energy levels in the island. It is much weaker than the response to the gate voltage, which is dominated by classical CB oscillations.

In this Letter, we demonstrate that, in ferromagnets with strong spin-orbit coupling, large chemical potential shifts can be induced by magnetization rotations leading to unprecedented characteristics of the ferromagnetic SET. The signatures of this Coulomb blockade anisotropic magnetoresistance (CBAMR) effect are MR signals which have magnitudes approaching the resistance variations due to CB oscillations, which can show both positive and negative hysteretic spin-valve-like characteristics controlled by the SET gate voltage and which occur at magnetic fields corresponding to ferromagnetic anisotropy fields.

Our SETs are fabricated from p-type (Ga, Mn)As, a ferromagnetic semiconductor for which parameters derived from the spin-orbit coupled band structure are known to be strongly anisotropic with respect to the magnetization orientation [7–13]. A schematic diagram of the device is shown in Fig. 1(a). The SET consists of a trench-isolated side-gated 40 nm wide channel aligned along the [110] direction. It was patterned by e-beam lithography and reactive ion etching in a 5 nm $Ga_{0.98}Mn_{0.02}As$ epilayer, which was grown along the [001] crystal axis on an AlAs buffer layer by low-temperature molecular beam epitaxy [12]. The narrow channel technique is a standard approach that has been used to produce nonmagnetic thin film Si and GaAs-based SETs in which disorder potential fluctuations create small islands in the channel without the need for a lithographically defined island [14,15]. These SETs are well suited for exploring functionalities based on classical single-electron charging effects on which we focus in this Letter. High precision electrical measurements were performed to exclude spurious effects associated with large changes in the resistance of the SETs. The dc currents were measured using subfemtoampere source-measure units at a constant source-drain voltage. Simultaneously, voltage drops over constricted and unstructured parts of the bar were detected using a potentiometric method which achieves impedances of the voltmeters larger than 1 GΩ.

Figure 1(b) shows clear CB oscillation diamonds [1] in the $V_G - V_{SD}$ plot, where V_{SD} is the source-drain voltage and V_G is the gate voltage. Consistent with the CB phe-

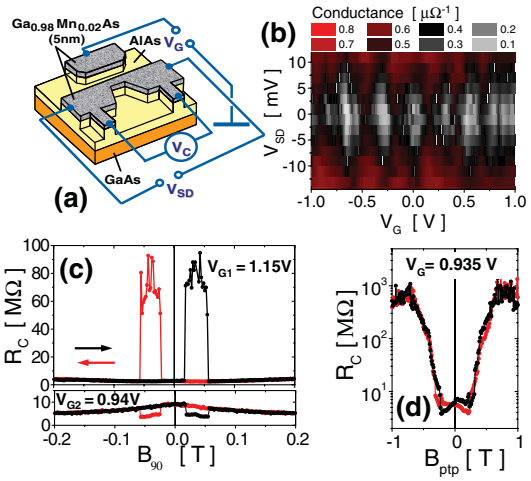

FIG. 1 (color). (a) Schematics of the CBAMR device. (b) CB conductance (I/V_C) oscillations with gate voltage for different source-drain bias. The diamond patterns in this 2D plot are clear fingerprints of single-electron transport. (c) Spin-valve-like MR signals of different magnitudes and opposite signs for gate voltages 1.15 and 0.94 V. Measurements were done in up and down sweeps of in-plane magnetic field B_{90} and at $V_{SD} = 3$ mV. (d) Huge MR signal for up and down sweeps of the perpendicular-to-plane magnetic field at $V_G = 0.935$ V.

nomenology, the width of the low conductance parts of the oscillations gradually decreases with increasing V_{SD} as the source-drain bias approaches the single-electron charging energy. We have investigated three different devices, all of which show the same qualitative behavior. Thermal cycling of the individual devices leads to only quantitative changes in the CB oscillation pattern as is typical of SETs realized in narrow channels [14,16].

All MR data in this Letter were measured at 4.2 K. Magnetic fields were applied in the plane of the film at an angle θ to the current I direction (B_θ) or in the perpendicular-to-plane direction (B_{ptp}). Examples of large, hysteretic, and gate-voltage dependent MRs of the SET are shown in Fig. 1(c) for up and down sweeps of the magnetic field B_{90}. At about 20 mT, the MR is ~100% and negative for $V_G = 0.94$ V but is larger than 1000% and positive for $V_G = 1.15$ V. The shape of the hysteretic MR curves in Fig. 1(c) is reminiscent of spin-coherent resonant tunneling at different relative orientations of magnetizations in individual parts of a magnetic SET, reported, e.g., in Refs. [3,6]. It is, however, extremely improbable that these subtle quantum effects play an important role in our narrow channel (Ga, Mn)As SETs with islands created by disorder potential fluctuations, and we also emphasize that the magnitude of our hysteretic and gate-controlled MRs is incomparably larger. Figure 1(d) shows very large MR at $V_G = 0.935$ V due to the rotation of magnetization out of the plane of the (Ga, Mn)As epilayer during magnetic field B_{ptp} sweeps. Resistance variations by more than 3 orders of magnitude are observed with the high resistance state realized at saturation. The striking sensitivity to the orientation of the applied magnetic field hints to the anisotropic MR origin of the effect we observe. This is confirmed by the observation of comparably large and gate-controlled MR in our devices when saturation magnetization is rotated with respect to the crystallographic axes. These measurements, presented in the following paragraph, also help to elucidate the microscopic origin of the CBAMR.

The anisotropic MR of our SET device is demonstrated in Figs. 2(c) and 2(d) and compared with normal anisotropic MR in the unstructured part of the (Ga, Mn)As bar, plotted in Figs. 2(a) and 2(b). Abrupt rotations via intermediate magnetization angles occur in the field sweep measurements [Figs. 2(a) and 2(c)] as a result of the combined uniaxial and cubic in-plane anisotropies present in the (Ga, Mn)As epilayer [17,18]. As suggested above, we refrain from speculating on the details of magnetization reversals at low fields in the individual parts of our SET and focus on its behavior at saturation where magnetizations of all magnetic parts of the device are aligned with the external field [11,12,19]. This is explored systematically in Figs. 2(b) and 2(d) for a 5 T rotating magnetic field whose magnitude is well above any observed anisotropy field in our devices. (Note that Lorentz force effects are negligible at these saturating fields, as the change in resistance with increasing magnetic field is independent of the field angle.) In the unstructured part of the bar, higher or lower resistance states correspond to magnetization along or perpendicular to the current direction, as seen from both Figs. 2(a) and 2(b). Similar behavior is seen in the SET part

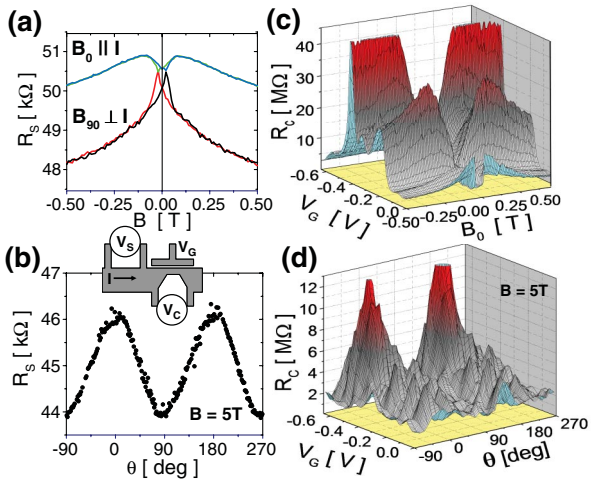

FIG. 2 (color). (a) Resistance $R_S = V_S/I$ of the unstructured bar (see schematic diagram) vs up and down sweeps of in-plane magnetic field parallel (blue/green) and perpendicular (red/black) to the current direction. (b) R_S vs the angle between the current direction and an applied in-plane magnetic field of 5 T, at which $\mathbf{M} \parallel \mathbf{B}$. (c) Channel resistance R_C vs gate voltage and down sweep of the magnetic field parallel to current. (d) R_C vs gate voltage and the angle between the current direction and an applied in-plane magnetic field of 5 T.

of the device at, for example, $V_G = -0.4$ V [see Figs. 2(c) and 2(d)], but the anisotropic MR is now hugely increased and depends strongly on the gate voltage.

Figure 3 demonstrates that the dramatic anisotropic MR effects in the SET are due to shifts in the CB oscillation pattern caused by the changes in magnetization orientation. The shifts are clearly seen in Fig. 3(a), which shows the CB oscillations for several magnetization angles. Blue curves indicate shifts in the oscillation pattern due to magnetization rotations. For example, at $V_G = -0.4$ V [highlighted in Fig. 3(a) by the red line] the oscillations have a peak for $\theta = 0°$ that moves to higher V_G with increasing θ until, for $\theta = 40°$, a minimum in the oscillatory resistance occurs at $V_G = -0.4$ V. Figures 3(a) and 3(b) show that the magnitude of the resistance variations with θ at fixed V_G and with V_G at fixed θ is comparable.

As we point out below in the theory discussion, the key parameters for the CBAMR effect are the magnetization rotation induced electrochemical shifts relative to the Coulomb blockade charging energy. The charging energy obtained from experimental data in Fig. 3(c) is ~4 meV. Note that the CB oscillation period inferred from data in Fig. 3(a) is ~100 mV. As the Coulomb blockade charging energy and oscillation period for a single island are $e^2/2C_\Sigma$ and e/C_G respectively, this implies that C_Σ, the total island capacitance, is much larger than C_G, the gate-island capacitance. The experimental value of C_Σ suggests that the characteristic size of the island is smaller than ~20 nm. These rough estimates show that more than one island in the 40 nm channel SET may be contributing, consistent with the observed complex CB oscillations.

We now analyze theoretically the microscopic origin of the CBAMR, which we attribute to the spin-orbit coupling induced anisotropy of the carrier chemical potential. As confirmed by detailed calculations below, we expect the nonuniform carrier concentration near the channel, implied by the existence of CB, to produce magnetization orientation dependent differences between chemical potentials of the lead and of the island in the constriction $\Delta\mu(\mathbf{M})$. The schematic cartoons in Fig. 4 indicate the contributions to the Gibbs energy associated with the transfer of charge Q from the lead to the island. The energy can be written as a sum of the internal, electrostatic charging energy term and the term associated with, in general, different chemical potentials of the lead and of the island: $U = \int_0^Q dQ' \Delta V_D(Q') + Q\Delta\mu/e$, where $\Delta V_D(Q) = (Q + C_G V_G)/C_\Sigma$. The Gibbs energy U is minimized for $Q_0 = -C_G(V_G + V_M)$, where the magnetization orientation dependent shift of the CB oscillations is given by $V_M = C_\Sigma/C_G\Delta\mu(\mathbf{M})/e$. Since $|C_G V_M|$ has to be of order $|e|$ to cause a marked shift in the oscillation pattern, the corresponding $|\Delta\mu(\mathbf{M})|$ has to be similar to e^2/C_Σ, i.e., of the order of the island single-electron charging energy. The fact that CBAMR occurs when the anisotropy in a band structure derived parameter is comparable to an independent scale (single-electron charging energy) makes the effect distinct and potentially much larger in magnitude as compared to the previously observed anisotropic MR in the Ohmic regime (normal AMR) and in the tunneling regime (TAMR) [9,11,13,19,20].

We have performed microscopic calculations to estimate chemical potential anisotropies in (Ga, Mn)As epilayers. We use the effective kinetic-exchange model that has been frequently employed to study these dilute magnetic moment p-type semiconductors, particularly the properties related to the strong spin-orbit coupling in the valence band [7–12]. The zero temperature calculations assume cubic magnetocrystalline anisotropy associated with the zinc-blende crystal structure plus an additional uniaxial

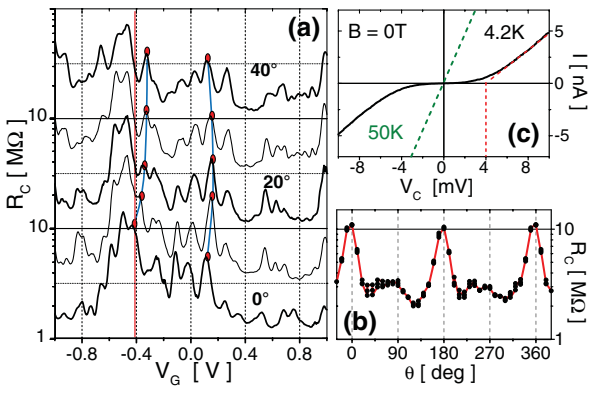

FIG. 3 (color). (a) Channel resistance vs gate voltage at in-plane saturation field of 5 T and several field angles θ. (b) θ sweep for fixed $V_G = -0.4$ V. (c) $I - V_C$ characteristic of the channel at 4.2 K (Coulomb blockade regime) and 50 K (Ohmic regime) used to determine the SET charging energy, as indicated by the red line. This inferred value remains constant with decreasing temperature below 4.2 K.

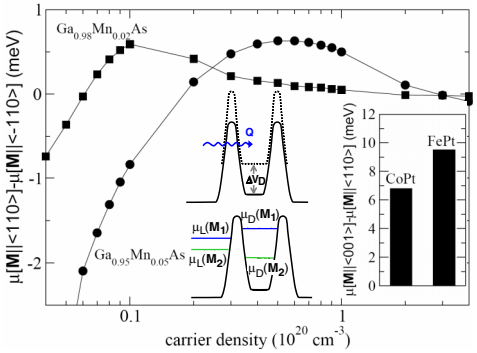

FIG. 4 (color online). Calculated chemical potential anisotropy in (Ga, Mn)As as a function of carrier density for Mn local moment concentrations of 2% and 5%. The uniaxial anisotropy is modeled by introducing a weak shear strain $e_{xy} = 0.001$. Insets: Schematics of the charging energy contribution (upper) to the Gibbs energy and the contribution proportional to the difference $\Delta\mu(\mathbf{M})$ in chemical potentials of the lead, $\mu_L(\mathbf{M})$, and of the island, $\mu_D(\mathbf{M})$ (lower); calculated chemical potential anisotropies in $L1_0$ FePt and CoPt ordered alloys.

field (as observed experimentally) modeled [18] by introducing a weak in-plane shear strain $e_{xy} = 0.001$. Numerical results are presented in Fig. 4 for two Mn concentrations and over a range of carrier concentrations where the higher values are expected to correspond to the leads and the lower values to the constricted part of the bar. The data confirm that the chemical potential anisotropies in ferromagnetic (Ga, Mn)As are sensitive to the carrier and local moment density and may even change sign and that $|\Delta\mu|$ of a few meV that would explain the measured CB oscillation shifts are plausible. Note that CBAMR as analyzed above can occur for either a ferromagnetic or paramagnetic island.

CBAMR should be generic to SETs fabricated in ferromagnetic systems with spin-orbit coupling. In ferromagnetic metals, highly accurate *ab initio* methods are available to study the spin-orbit coupled spectral properties. Recently, the technique has been successfully applied to describe magnetocrystalline anisotropies in $L1_0$ FePt and CoPt ordered alloys and to predict the existence of the TAMR effect in transition metal tunnel junctions [21–24]. FePt and CoPt are useful model systems with both large exchange splitting resulting in the Curie temperatures well above room temperature and strong spin-orbit coupling. The calculated chemical potential anisotropies, shown in the inset in Fig. 4, are roughly an order of magnitude larger than in (Ga, Mn)As. This suggests that metal-based ferromagnetic SETs may offer a route to the high temperature CBAMR effect.

To conclude, we have observed a new type of MR effect, CBAMR, in a ferromagnetic semiconductor SET and explained its origin in terms of electrochemical shifts that are anisotropic with respect to the magnetization orientation. The effect should be generic and offers new functionality concepts combining electrical transistorlike action with permanent information storage or utilizing magnetization controlled transistor characteristics in a single nanoscale element.

The authors acknowledge discussions with Allan MacDonald and Jairo Sinova and support from the EPSRC through Grant No. GR/S81407/01, from the Grant Agency and Academy of Sciences of the Czech Republic through Grants No. 202/05/0575 and No. AV0Z10100521, and from the Ministry of Education of the Czech Republic Grant No. LC510.

[1] K. K. Likharev, Proc. IEEE **87**, 606 (1999).
[2] S. A. Wolf, D. D. Awschalom, R. A. Buhrman, J. M. Daughton, S. von Molnár, M. L. Roukes, A. Y. Chtchelkanova, and D. M. Treger, Science **294**, 1488 (2001).
[3] K. Ono, H. Shimada, and Y. Ootuka, J. Phys. Soc. Jpn. **66**, 1261 (1997).
[4] M. M. Deshmukh and D. C. Ralph, Phys. Rev. Lett. **89**, 266803 (2002).
[5] A. N. Pasupathy, R. C. Bialczak, J. Martinek, J. E. Grose, L. A. K. Donev, P. L. McEuen, and D. C. Ralph, Science **306**, 86 (2004).
[6] S. Sahoo, T. Kontos, J. Furer, C. Hoffmann, M. Gräber, A. Cottet, and C. Schönenberger, Nature Phys. **1**, 99 (2005).
[7] T. Dietl, H. Ohno, F. Matsukura, J. Cibert, and D. Ferrand, Science **287**, 1019 (2000).
[8] M. Abolfath, T. Jungwirth, J. Brum, and A. H. MacDonald, Phys. Rev. B **63**, 054418 (2001).
[9] T. Jungwirth, J. Sinova, K. Y. Wang, K. W. Edmonds, R. P. Campion, B. L. Gallagher, C. T. Foxon, Q. Niu, and A. H. MacDonald, Appl. Phys. Lett. **83**, 320 (2003).
[10] L. Brey, C. Tejedor, and J. Fernández-Rossier, Appl. Phys. Lett. **85**, 1996 (2004).
[11] C. Gould, C. Rüster, T. Jungwirth, E. Girgis, G. M. Schott, R. Giraud, K. Brunner, G. Schmidt, and L. W. Molenkamp, Phys. Rev. Lett. **93**, 117203 (2004).
[12] A. D. Giddings *et al.*, Phys. Rev. Lett. **94**, 127202 (2005).
[13] H. Saito, S. Yuasa, and K. Ando, Phys. Rev. Lett. **95**, 086604 (2005).
[14] M. A. Kastner, Rev. Mod. Phys. **64**, 849 (1992).
[15] K. Tsukagoshi, B. W. Alphenaar, and K. Nakazato, Appl. Phys. Lett. **73**, 2515 (1998).
[16] As expected, Coulomb staircase effects, i.e., quasiperiodic fluctuations, in dI/dV_{SD} vs V_{SD} related to the multiple-electron tunneling through the dot are not well pronounced in our data. These oscillations can be strong in lithographically defined SETs with large differences between resistances of tunnel barriers separating the island and the two leads [1].
[17] K. Y. Wang, K. W. Edmonds, R. P. Campion, L. X. Zhao, C. T. Foxon, and B. L. Gallagher, Phys. Rev. B **72**, 085201 (2005).
[18] M. Sawicki *et al.*, Phys. Rev. B **71**, 121302(R) (2005).
[19] C. Ruester, C. Gould, T. Jungwirth, J. Sinova, G. M. Schott, R. Giraud, K. Brunner, G. Schmidt, and L. W. Molenkamp, Phys. Rev. Lett. **94**, 027203 (2005).
[20] F. Matsukura, M. Sawicki, T. Dietl, D. Chiba, and H. Ohno, Physica (Amsterdam) **21E**, 1032 (2004).
[21] A. B. Shick and O. N. Mryasov, Phys. Rev. B **67**, 172407 (2003).
[22] A. B. Shick, F. Máca, J. Mašek, and T. Jungwirth, Phys. Rev. B **73**, 024418 (2006).
[23] K. I. Bolotin, F. Kuemmeth, and D. C. Ralph, cond-mat/0602251.
[24] M. Viret, M. Gabureac, F. Ott, C. Fermon, C. Barreteau, and R. Guirado-Lopez, cond-mat/0602298.